



Begell House, Inc. Publishers

Journal Production

50 Cross Highway

Redding, CT 06896

Phone: 1-203-938-1300

Fax: 1-203-938-1304

Begell House Production Contact : journals@begellhouse.com

Dear Corresponding Author,

Attached is the corresponding author pdf file of your article that has been published.

Please note that the pdf file provided is for your own personal use and is not to be posted on any websites or distributed in any manner (electronic or print). Please follow all guidelines provided in the copyright agreement that was signed and included with your original manuscript files.

Any questions or concerns pertaining to this matter should be addressed to journals@begellhouse.com

Thank you for your contribution to our journal and we look forward to working with you again in the future.

Sincerely,

Michelle Amoroso

Michelle Amoroso

Production Department

TIME-DEPENDENT FLOW IN A COMPOSITE CHANNEL WITH HEAT TRANSFER

Muhammad Nasir,^{1,*} Sufian Munawar,^{1,2} & Asif Ali¹

¹Department of Mathematics Quaid-i-Azam University, Islamabad, Pakistan 44000

²Department of Mathematics, School of Science and Technology, University of Management and Technology, Lahore Pakistan 54000

*Address all correspondence to Muhammad Nasir E-mail: nasirmaths1@yahoo.com

Original Manuscript Submitted: 6/15/2012; Final Draft Received: 2/19/2013

In this article, unsteady oscillatory flow and heat transfer in a horizontal composite porous channel is discussed. The Darcy-Brinkman model is used to develop the governing equations for the flow in a porous medium. The upper plate is oscillating with the constant amplitude while the lower plate is stationary. The viscous and Darcian dissipation terms are included in the energy equation. At the interface of both regions the velocity, shear stress, and temperature profiles are assumed to be continuous. The governing equations for momentum and heat transfer are solved analytically using the series solution in terms of harmonic and nonharmonic functions in both regions of the channel. The effects of various physical parameters on the velocity and the temperature profiles are analyzed with the help of graphs and tables.

KEY WORDS: composite channel, oscillatory flow, heat transfer, interface boundary conditions, analytic solution

1. INTRODUCTION

In recent years, considerable interest has been developed in the study of flow and heat transfer characteristics in the channels with porous medium because of the significance and diversity of this research area in various engineering and geophysical applications. The applications include problems in thermal insulation, heat exchangers, geothermal reservoirs, and nuclear waste repositories.

The problem of flow in a channel was first investigated by Berman (1953) who discussed steady-state two-dimensional laminar flow of a viscous fluid in a channel consisting of two porous walls. Afterwards, Kim et al. (1994) described the pulsating flow and heat transfer in a channel filled with a porous medium. An enhanced heat transfer in an annular duct partially filled with a porous medium with high permeability and conductivity was investigated by Chikh et al. (1995) using the Brinkman model. Umavathi et al. (2005) considered the problem of unsteady oscillatory flow and heat transfer of two viscous immiscible fluids through a horizon-

tal channel with isothermal permeable walls. Umavathi (2011) analyzed a fully developed free convection flow of immiscible fluids in a vertical channel filled with a porous medium. Chauhan and Kumar (2012) considered the unsteady flow produced by an oscillatory motion of the lower plate in a horizontal porous layer. Li et al. (2010) numerically studied the fluid flow and heat transfer characteristics in a channel with staggered porous blocks. Usman et al. (2011) studied the behavior of unsteady magnetohydrodynamic (MHD) micropolar fluid flow and mass transfer past a vertical plate with variable suction. Umavathi et al. (2010) considered unsteady oscillatory flow and heat transfer of porous media sandwiched between two viscous fluids through a horizontal channel and the flow in porous medium was modeled using the Brinkman equation. Guo et al. (1997) adopted the Brinkman-Forchheimer-extended Darcy model for the porous matrix region of pulsating flow and heat transfer in a circular pipe. Chauhan and Kumar (2010, 2011) studied Couette flow and effects of heat transfer in a three-dimensional Couette flow through a composite porous

NOMENCLATURE

$$\chi = \begin{cases} 1 & \text{for porous matrix} \\ 0 & \text{for clear fluid} \end{cases}$$

$$\chi_{\mu} = \begin{cases} \mu_{eff} & \text{is the viscosity for porous matrix} \\ \mu & \text{is the viscosity for clear fluid} \end{cases}$$

$$\chi_k = \begin{cases} K_{eff} & \text{is the thermal conductivity for porous matrix} \\ K & \text{is the thermal conductivity for clear fluid} \end{cases}$$

channel which was partially filled with a porous medium. Gireesha et al. (2012) focused on the mathematical modeling of three-dimensional Couette flow and heat transfer of a dusty fluid between two infinite horizontal parallel porous plates. Khan et al. (2010) considered steady flow and heat transfer of a Sisko fluid in annular pipe and both analytical and numerical solutions of the governing nonlinear differential equations were presented. Umavathi et al. (2009) studied unsteady oscillatory flow and heat transfer in a horizontal composite porous channel using the Darcy- Brinkman equation. Leong and Jin (2005) conducted an experimental study on the heat transfer of oscillating flow through a channel filled with aluminum foam subjected to a constant wall heat flux. Andersson and Holmedal (1995) calculated exact analytical solutions in terms of infinite series expansions that were obtained for the start-up flow in a porous medium channel. Kaviany (1985) considered laminar flow through a porous channel bounded by two parallel plates maintained at a constant and equal temperature. An exact solution describing the fluid mechanics at the interface between a fluid layer and a porous medium was discussed by Vafai and Kim (1990). Huang and Vafai (1994) presented a numerical investigation for forced convection in an isothermal channel with porous cavity and block. Kuznetsov (2000) investigated fluid flow and heat transfer analysis of Couette flow in a composite duct. Kuznetsov (1997) discussed the analytical solution for the study of fluid flow in the interface region between a porous medium and a clear fluid in a channel partially filled with a porous medium. Analytical solution of the Couette flow in a composite channel was also discussed by Kuznetsov (1998).

In the present work, we have analyzed the unidirectional oscillatory flow in a channel of half porous space

with oscillatory upper plate. Continuous velocities and shear stresses are assumed at the interface of porous medium and clear fluid. An analytic series solution is calculated for the complete analysis of the velocity and the temperature profiles. Effects of sinusoidal oscillatory plate on the flow and the heat transfer in a composite porous medium are analyzed through graphical illustration.

2. MATHEMATICAL FORMULATION

Consider the unsteady fully developed laminar flow of an incompressible viscous fluid in an infinitely long composite channel. The region 1 ($-h < y < 0$) is filled with a porous matrix and the region 2 ($0 < y < h$) is filled with a clear viscous fluid. The upper wall of the channel is held at a constant temperature T_{w1} and the temperature at the lower wall of the channel is T_{w2} with $T_{w1} > T_{w2}$. As we are assuming the plates of the channel to be infinite and are placed horizontally along the x -axis, all of the physical variables except pressure depend on y and t only. Further, the flow in both regions of the channel is supposed to be driven by a constant pressure gradient $\partial p/\partial z$. At time $t = 0$, both the plates are assumed to be at rest and suddenly (at $t > 0$) the upper plate starts its motion with velocity $U = u_0 (1 + \epsilon A e^{i\omega t})$. Under these assumptions the governing equations of motion and the heat transfer are

$$\rho \left(\frac{\partial u_i}{\partial t} \right) = -\frac{\partial p}{\partial z} + \chi_{\mu} \left(\frac{\partial^2 u_i}{\partial y^2} \right) - \chi \frac{\mu}{s} u_i, \quad (1)$$

$$\rho C_p \left(\frac{\partial T_i}{\partial t} \right) = \chi_k \frac{\partial^2 T_i}{\partial y^2} - \chi_{\mu} \left(\frac{\partial u_i}{\partial y} \right)^2 + \chi \frac{\mu}{s} u_i^2 \quad (2)$$

where the index $i = 1$ gives equations for regions 1 and $i = 2$ gives equations for regions 2; u_i is the x -component of fluid velocity and T_i is the temperature field; ρ , μ , and C_p are the fluid density, dynamic viscosity, and specific heat at constant pressure, respectively; and s is the permeability of porous medium.

No-slip boundary conditions are taken into account for the velocity field and isothermal boundaries are assumed for temperature profile. Moreover, the velocity, the temperature and the shear stress at the interface point are continuous.

The boundary and interface conditions can then be written as

$$\begin{aligned} u_1(-h) &= 0, \quad T_1(-h) = T_{w1}, \\ u_2(h) &= U = u_0(1 + \epsilon A e^{i\omega t}), \quad T_2(h) = T_{w2}, \end{aligned} \quad (3)$$

$$\begin{aligned} u_1(0) &= u_2(0), \quad \mu_{eff} \frac{\partial u_1}{\partial y} = \mu \frac{\partial u_2}{\partial y}, \\ T_1(0) &= T_2(0), \quad K_{eff} \frac{\partial T_1}{\partial y} = K \frac{\partial T_2}{\partial y}, \end{aligned} \quad \text{at } y = 0. \quad (4)$$

where ω is the frequency parameter, A a real positive constant, and ϵ the amplitude, such that $\epsilon A < 1$.

We introduce the non-dimensional variables as

$$y^* = \frac{yu_0}{\nu}, \quad u_i^* = \frac{u_i}{u_0}, \quad t^* = \frac{tu_0^2}{\nu}, \quad \theta = \frac{T - T_{w2}}{T_{w1} - T_{w2}}. \quad (5)$$

Using (5) and dropping the asterisk for simplicity, Eqs. (1) and (2) in dimensionless form become

$$\frac{\partial u_i}{\partial t} = -P + A_i \frac{\partial^2 u_i}{\partial y^2} - \chi \sigma^2 u_i, \quad (6)$$

$$\frac{\partial \theta_i}{\partial t} = B_i \frac{\partial^2 \theta_i}{\partial y^2} + Ec A_i \left(\frac{\partial u_i}{\partial y} \right)^2 + \chi Ec \sigma^2 u_i^2, \quad (7)$$

where $A_1 = m$, $A_2 = 1$, $B_1 = k/Pr$, $B_2 = 1/Pr$, $P = [\mu/(\rho^2 u_0^3)][(\partial p)/(\partial z)]$, $Pr = \rho \nu C_p/k$ is the Prandtl number; $m = \mu_{eff}/\mu$ is the ratio of viscosities and $k = K_{eff}/K$ is the ratio of thermal conductivities; $\sigma^2 = \nu^2/(su_0^2)$ is the porosity parameter; and $Ec = u_0^2/C_p \Delta T$ is the Eckert number.

The boundary and interface conditions reduce to

$$\begin{aligned} u_1(-1) &= 0, \quad u_2(1) = 1 + \epsilon A e^{i\omega t}, \\ \theta_1(-1) &= 1, \quad \theta_2(1) = 0, \end{aligned} \quad (8)$$

$$\begin{aligned} u_1(0) &= u_2(0), \quad \theta_1(0) = \theta_2(0), \\ m \frac{\partial u_1}{\partial y} \Big|_{y=0} &= \frac{\partial u_2}{\partial y} \Big|_{y=0}, \quad k \frac{\partial \theta_1}{\partial y} \Big|_{y=0} = \frac{\partial \theta_2}{\partial y} \Big|_{y=0}. \end{aligned} \quad (9)$$

3. SOLUTION OF THE PROBLEM

The momentum and the energy Eqs. (6) and (7), respectively, are coupled partial differential equations that cannot be solved in closed form easily. However, these partial differential equations can be reduced to a set of ordinary differential equations that can be solved analytically by expanding the series for velocity and temperature fields as

$$\begin{aligned} u_i(y, t) &= u_{i0}(y) + \epsilon e^{i\omega t} u_{i1}(y) + O(\epsilon^2) \dots, \\ \text{for } i &= 1, 2, \end{aligned} \quad (10)$$

$$\begin{aligned} \theta_i(y, t) &= \theta_{i0}(y) + \epsilon e^{i\omega t} \theta_{i1}(y) + O(\epsilon^2) \dots \\ \text{for } i &= 1, 2. \end{aligned} \quad (11)$$

This is a valid assumption because of the choice of u_i at the upper boundary as defined in Eq. (3) with the condition that $\epsilon A < 1$. By substituting Eqs. (10) and (11) into Eqs. (8) and (9), equating the harmonic and nonharmonic terms, and neglecting the terms of order $O(\epsilon^2)$ and higher, one can obtain the following pairs of equations for (u_{i0}, θ_{i0}) and (u_{i1}, θ_{i1}) .

Non-periodic coefficients $O(\epsilon^0)$:

$$A_i \frac{\partial^2 u_{i0}}{\partial y^2} - \chi \sigma^2 u_{i0} = P, \quad (12)$$

$$B_i \frac{\partial^2 \theta_{i0}}{\partial y^2} + Ec A_i \left(\frac{\partial u_{i0}}{\partial y} \right)^2 + \chi Ec \sigma^2 u_{i0}^2 = 0. \quad (13)$$

Periodic coefficients $O(\epsilon^1)$:

$$A_i \frac{\partial^2 u_{i1}}{\partial y^2} - \chi \sigma^2 u_{i1} - i\omega u_{i1} = 0, \quad (14)$$

$$\begin{aligned} B_i \frac{\partial^2 \theta_{i1}}{\partial y^2} - i\omega \theta_{i1} + 2Ec A_i \left(\frac{\partial u_{i0}}{\partial y} \right) \left(\frac{\partial u_{i1}}{\partial y} \right) \\ + 2\chi Ec \sigma^2 u_{i0} u_{i1} = 0. \end{aligned} \quad (15)$$

Using Eqs. (10) and (11), the boundary and interface conditions can be written as

$$\begin{aligned} u_{1i}(-1) &= 0, \quad u_{20}(1) = 1, \quad u_{21}(1) = A, \\ u_{1i}(0) &= u_{2i}(0), \end{aligned} \quad (16)$$

$$m \frac{\partial u_{1i}}{\partial y} = \frac{\partial u_{2i}}{\partial y} \quad \text{at } y = 0, \quad (17)$$

$$\theta_{1i}(-1) = 1 - \delta_{1i}, \quad \theta_{2i}(1) = 0, \quad (18)$$

$$\theta_{1i}(0) = \theta_{2i}(0), \quad k \frac{\partial \theta_{1i}}{\partial y} = \frac{\partial \theta_{2i}}{\partial y} \quad \text{at } y = 0. \quad (19)$$

where $i = 0, 1$ gives the boundary and interface conditions for non-periodic $O(\epsilon^0)$ and periodic $O(\epsilon^1)$ coefficients, respectively, and δ_{1i} is the Kronecker delta.

4. RESULTS AND DISCUSSION

The non-linear differential Eqs. (12)–(15) with boundary conditions (16)–(19) are solved analytically. The closed-form solutions are valid within the range $\epsilon A < 1$. As the solutions of these equations are lengthy and complicated, for simplicity we are giving only tabulated values for the velocity and temperature profiles and their derivatives in Table 1.

The graphical results of the obtained analytical solutions are discussed. The effects of various physical parameters on the velocity and temperature profiles are illustrated in Figs. 1–13.

The effects of the viscosity ratio parameter m on the velocity and temperature profiles are shown in Figs. 1 and 2. It is observed from the figures that as m increases the velocity and the temperature profile decrease significantly. This conduct of the flow is due to the thickness of the fluid for which the process of convection becomes slow and hence the velocity and the temperature profiles decrease. It is worth mentioning here that the velocity profile in the porous region is small as compared to the clear region. This shows that the momentum transport in the porous region is small due to the presence of a large resistive force.

The effects of pressure gradients on the velocity and the temperature profiles are shown in Figs. 3 and 4. Obviously, the velocity profile increases by increasing the

TABLE 1: Numerical values of velocity and temperature profiles and their derivatives by taking various values of y between -1 and 1 while $\sigma = 1$, $m = 0.25$, $P = -1$, $\omega = 1$, $\omega t = \pi/3$, $k = 0.25$, $Ec = 2$, $Pr = 0.1$ and $\epsilon A = 0.2$ are kept fixed

y	u	u'	θ	θ'
-1	0	2.26906	1.0	-0.54259
-0.8	0.384929	1.63135	0.880033	-0.6459
-0.6	0.670004	1.25695	0.743853	-0.71403
-0.4	0.900958	1.08226	0.594474	-0.78053
-0.2	1.1139	1.07318	0.431274	-0.85220
0.0	1.34045	1.21803	0.253479	-0.92549
0.2	1.38003	0.0908022	0.207165	-0.23218
0.4	1.37657	-0.125994	0.160317	-0.23734
0.6	1.32936	-0.346773	0.11168	-0.25072
0.8	1.23753	-0.572446	0.0592069	-0.27641
1.0	1.1	-0.803906	1.562×10^{-9}	-0.31882

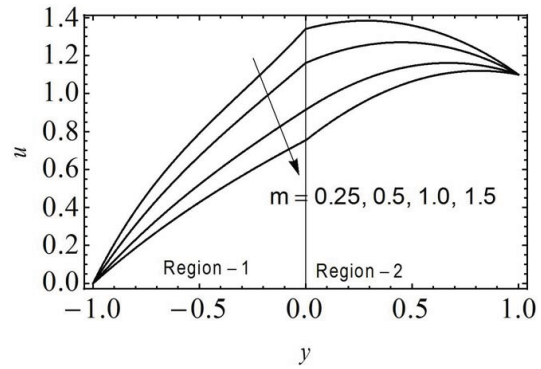


FIG. 1: The velocity profile for different values of the ratio of viscosities m , when $\sigma = 1$, $P = -1$, $\omega = 1$, $\omega t = \pi/3$, $\epsilon A = 0.2$ are kept fixed

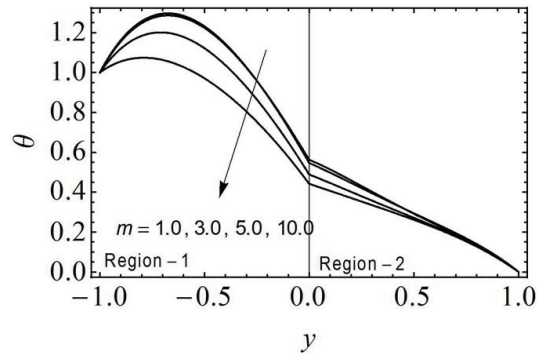


FIG. 2: The temperature profile for different values of the ratio of viscosities m , when $\sigma = 1$, $P = -2$, $\omega = 1$, $\omega t = \pi/3$, $\epsilon A = 0.2$, $Ec = 2$, $Pr = 0.2$, $k = 0.25$ are kept fixed

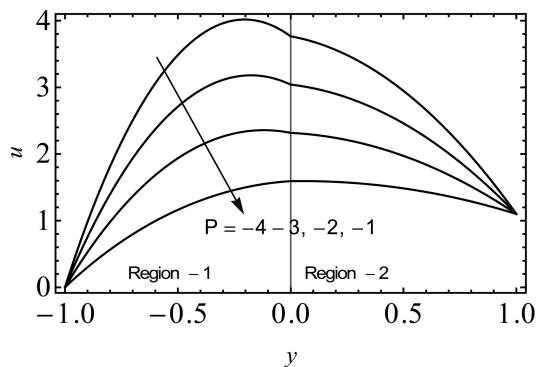


FIG. 3: The velocity profile for different values of pressure gradient P , when $\sigma = 1$, $m = 1$, $\omega = 1$, $\omega t = \pi/3$, $\epsilon A = 0.2$ are kept fixed

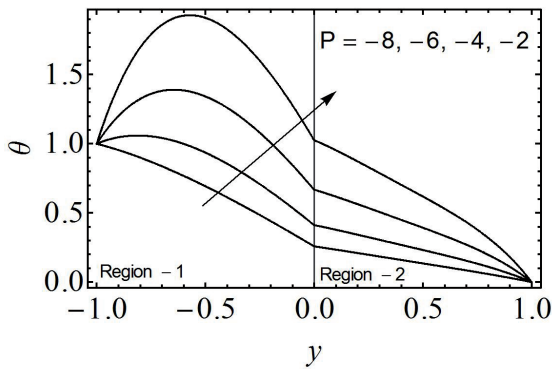


FIG. 4: The temperature profile for different values of pressure gradient P , when $\sigma = 1$, $\omega = 1$, $\omega t = \pi/3$, $\epsilon A = 0.2$, $Ec = 2$, $Pr = 0.1$, $k = 0.25$ are kept fixed

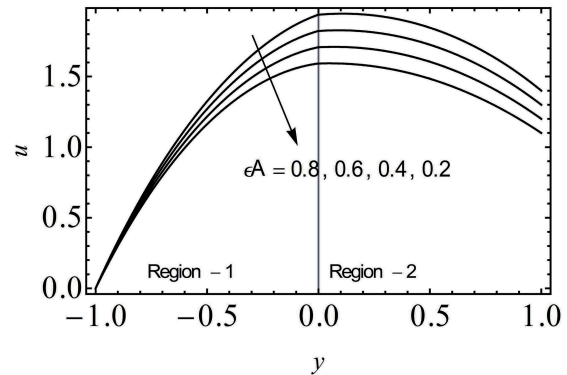


FIG. 7: The velocity profile for different values of ϵA , when $\sigma = 1$, $m = 1$, $P = -1$, $\omega = 1$, $\omega t = \pi/3$ are kept fixed

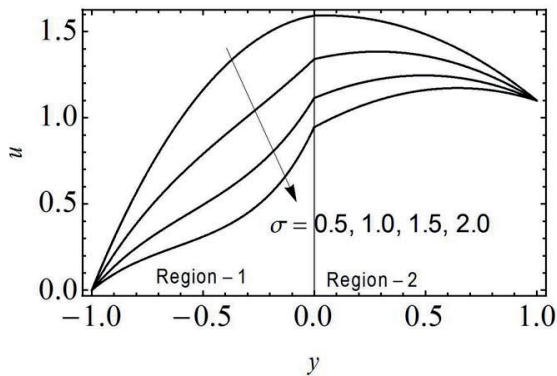


FIG. 5: The velocity profile for different values of the porosity parameter σ , when $m = 1$, $P = -1$, $\omega = 1$, $\omega t = \pi/3$, $\epsilon A = 0.2$ are kept fixed

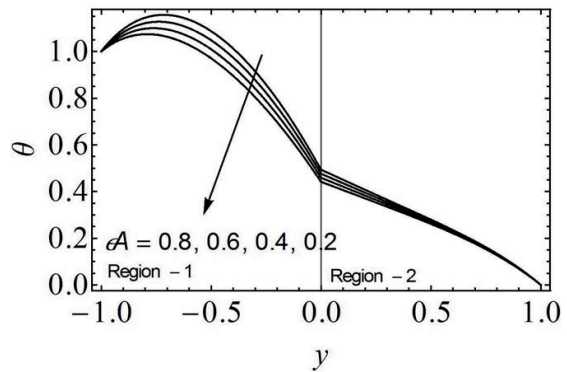


FIG. 8: The temperature profile for different values of ϵA , when $m = 1$, $\sigma = 1$, $\omega = 1$, $\omega t = \pi/3$, $Ec = 2$, $Pr = 0.2$, $k = 0.25$ are kept fixed

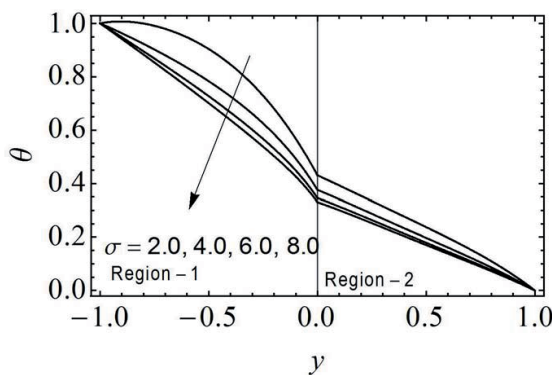


FIG. 6: The temperature profile for different values of the porosity parameter σ , when $m = 1$, $\omega = 1$, $\omega t = \pi/3$, $\epsilon A = 0.2$, $Ec = 2$, $Pr = 0.1$, $k = 0.25$ are kept fixed

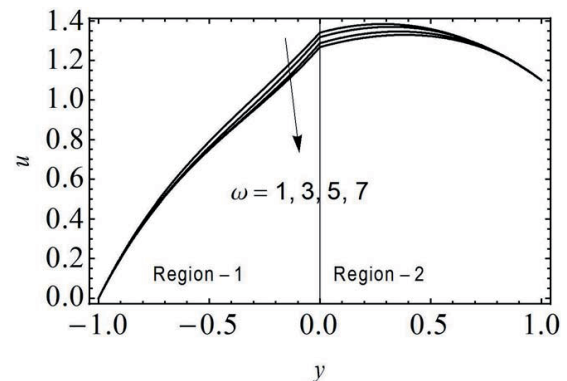


FIG. 9: The velocity profile for different values of angular frequency ω , when $\sigma = 1$, $P = -1$, $m = 1$, $\omega t = \pi/3$, $A = 1$ are kept fixed

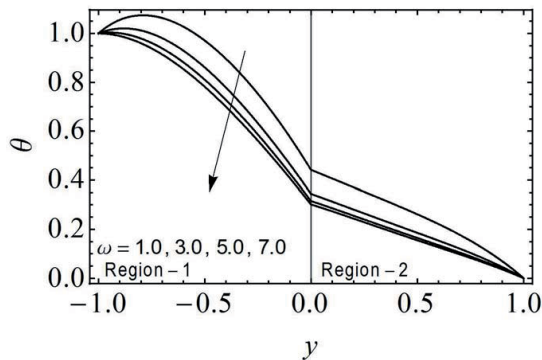


FIG. 10: The temperature profile for different values of angular frequency ω , when $m = 1$, $\sigma = 1$, $\omega t = \pi/3$, $Ec = 2$, $Pr = 0.1$, $k = 0.25$ are kept fixed

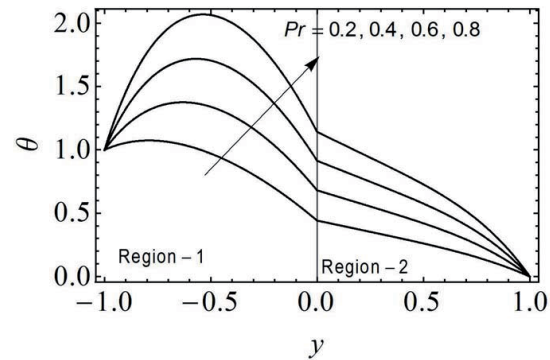


FIG. 13: The temperature profile for different values of the ratio of the Prandtl number Pr , when $\sigma = 1.0$, $P = -2.0$, $\omega = 1$, $\omega t = \pi/3$, $k = 0.25$, $Ec = 2$, $m = 1$ are kept fixed

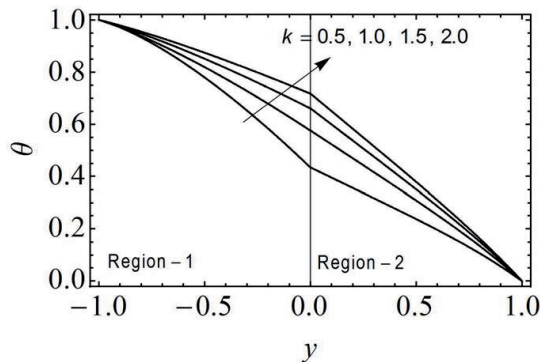


FIG. 11: The temperature profile for different values of the ratio of the conductivities k , when $\sigma = 1.0$, $P = -2$, $\omega = 1$, $\omega t = \pi/3$, $Pr = 0.1$, $Ec = 2$, $m = 1$ are kept fixed

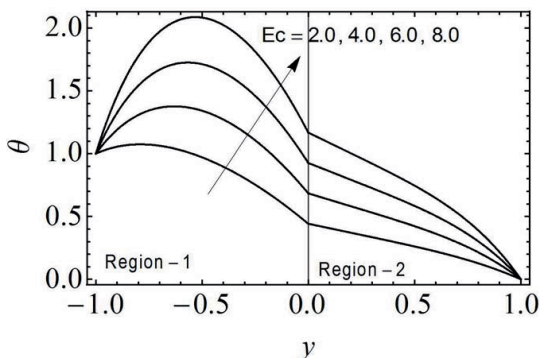


FIG. 12: The temperature profile for different values of the ratio of the Eckert number Ec , when $\sigma = 1.0$, $P = -2.0$, $\omega = 1$, $\omega t = \pi/3$, $Pr = 0.1$, $k = 0.25$, $m = 1$ are kept fixed

favorable pressure gradient. The temperature profile also augments as the favorable pressure gradient increases, which is only due to the augmentation of the phenomenon of convection.

Figures 5 and 6 demonstrate the effects of porosity parameter σ on the velocity and the temperature profiles. The large value of σ corresponds to small permeability. It is noticed from the figures that both the velocity and temperature profile decrease as σ increases in both regions. However, it is noted that this decrease in the velocity and temperature profiles is more prominent in the region 1 than that of the region 2 which is due to the occurrence of a large resistive force in region 1.

Figures 7 and 8 show the effects of amplitude of oscillations of the upper plate on the velocity and the temperature profiles. Here we can see that as ϵA increases the velocity profile also increases near the upper plate but this increase is not significant in the region 1. This behavior is expected because as the upper plate oscillates with high amplitude, the velocity of the particles near the upper plate also enhances. The temperature profile also increases as the amplitude of oscillation increases, although this increase is more significant in region 1 as compared to region 2.

Figures 9 and 10 show the velocity and the temperature profiles for different values of angular frequency ω . From here we note that by increasing angular frequency ω , the velocity and temperature profiles decrease.

Figure 11 illustrates the graph of the temperature profile for the different values of k . It is noticed from the figure that as the value of k increases the temperature profile also increases significantly. This is quite expected behavior.

ior of the temperature profile on increasing the thermal conductance of the fluid. Figure 12 depicts the effect of the Eckert number Ec on the temperature profile. Physically, the Eckert number represents the effect of the viscous dissipations in the fluid. It is observed from the figure that as Ec increases the temperature profile also increases which is because of the increasing heat due to fluid frictional effects. Figure 13 represents the effect of the Prandtl number Pr on the temperature profile. It is observed that the temperature increases as the Pr number increases. This conduct of the temperature profile is due to increase of viscous diffusivity in the fluid in the presence of viscous dissipation.

5. CONCLUSION

An unsteady flow of a viscous fluid between two parallel infinite plates whose half space is filled with porous medium and whose upper plate is oscillating is analyzed analytically. Solutions for the flow and the heat transfer equations are plotted graphically for various physical parameters, and the following observations are concluded from the above analysis:

- The behavior of the velocity and the temperature profiles is the same for various physical parameters.
- Both the temperature and the velocity profiles decrease as the ratio of viscosities increases in both regions.
- The favorable pressure gradient helps in the augmentation of the process of convection.
- It is observed that the velocity profile increases near the oscillating plate more significantly as compared to the lower plate when the amplitude of oscillations increases.
- Velocity and temperature decrease with the increase of angular frequency. The temperature profile also increases with the increase of oscillation amplitude.
- It is also noticed that the temperature profile is an increasing function of the Prandtl number, the Eckert number, and the thermal conductivity.

ACKNOWLEDGMENT

The authors are grateful to the reviewers of the paper for their valuable comments and suggestions for improving the quality of the manuscript.

REFERENCES

- Andersson, H. I. and Holmedal, L. E., Start-up flow in a porous medium channel, *Acta Mech.*, vol. **113**, pp. 155–168, 1995.
- Berman, A. S., Laminar flow in channels with porous walls, *J. Appl. Phys.*, vol. **24**, pp. 1232–1235, 1953.
- Chikh, S., Boumediene, A., Bouhadeif, K., and Lauriat, G., Analytical solution of non-Darcian forced convection in an annular duct partially filled with a porous medium, *Int. J. Heat Mass Transfer*, vol. **38**, pp. 1543–1551, 1995.
- Chauhan, D. S. and Kumar, V., Radiation effects on steady flow through a porous medium channel with velocity and temperature slip boundary conditions, *Appl. Math. Sci.*, vol. **6**, pp. 1759–1769, 2012.
- Chauhan, D. S. and Kumar, V., Heat transfer in a Couette flow through a composite channel partly filled by a porous medium with a transverse sinusoidal injection velocity and heat source, *Therm. Sci.*, vol. **15**, pp. 175–186, 2011.
- Chauhan, D. S. and Kumar, V., Three dimensional Couette flow in a composite channel partially filled with a porous medium, *Appl. Math. Sci.*, vol. **4**, pp. 2683–2695, 2010.
- Gireesha, B. J., Chamkha, A. J., Vishalakshi, C. S., and Bagewadi, C. S., Three-dimensional Couette flow of a dusty fluid with heat transfer, *Appl. Math. Modell.*, vol. **36**, pp. 683–701, 2012.
- Guo, Z., Kim, S. Y., and Sung, H. J., Pulsating flow and heat transfer in a pipe partially filled with a porous medium, *Int. J. Heat Mass Transfer*, vol. **40**, pp. 4209–4218, 1997.
- Huang, P. C. and Vafai, K., Internal heat transfer augmentation in a channel using an alternate set of porous cavity-block obstacles, *Int. J. Comput. Meth.*, vol. **25**, pp. 519–539, 1994.
- Kaviany, M., Laminar flow through a porous channel bounded by two parallel plates *Int. J. Heat Mass Transfer*, vol. **28**, pp. 851–858, 1985.
- Khan, M., Munawar, S., and Abbasbandy, S., Steady flow and heat transfer of a Sisko fluid in annular pipe, *Int. J. Heat Mass Transfer*, vol. **53**, pp. 1290–1297, 2010.
- Kim, S. Y., Kang, B. H., and Hyum, J. M., Heat Transfer from pulsating flow in a channel filled with porous media *Int. J. Heat Mass Transfer*, vol. **37**, pp. 2025–2033, 1994.
- Kuznetsov, A. V., Fluid flow and heat transfer analysis of Couette flow in a composite duct, *Acta Mech.*, vol. **140**, pp. 163–170, 2000.
- Kuznetsov, A. V., Influence of the stress jump condition at the porous/clear fluid interface on a flow at a porous wall, *Int. Commun. Heat Mass Transfer*, vol. **24**, pp. 401–410, 1997.
- Kuznetsov, A. V., Analytical investigation of Couette flow in a composite channel partially filled with a porous medium and partially filled with a clear fluid, *Int. J. Heat Mass Transfer*, vol. **41**, pp. 2556–2560, 1998.

- Leong, K. C. and Jin, L. W., An experimental study of heat transfer in oscillating flow through a channel filled with an aluminum foam, *Int. J. Heat Mass Transfer*, vol. **48**, pp. 243–253, 2005.
- Li, H. Y., Leong, K. C., Jin, L. W., and Chai, J. C., Analysis of fluid flow and heat transfer in a channel with staggered porous blocks, *Int. J. Therm. Sci.*, vol. **49**, pp. 950–962, 2010.
- Umavathi, J. C., Chakha, J. A., Mateen, A., and Al-Mudhaf, A., Unsteady two-fluid flow and heat transfer in a horizontal channel, *Int. J. Heat Mass Transfer*, vol. **42**, pp. 81–90, 2005.
- Umavathi, J. C., free convection of composite porous medium in a vertical channel, *Heat Transfer—Asian Res.*, vol. **40**, pp. 308–329, 2011.
- Umavathi, J. C., Liu, I. C., Prathap-Kumar, J., and Shaik-Meera, D., Unsteady flow and heat transfer of porous media sandwiched between viscous fluids, *Appl. Math. Mech.*, vol. **31**, pp. 1497–1516, 2010.
- Umavathi, J. C., Chamkha, A. J., Mateen, A., and Al-Mudhaf, A., Unsteady oscillatory flow and heat transfer in a horizontal composite porous medium channel, *Nonlinear Anal. Modell. Control*, vol. **14**, pp. 397–415, 2009.
- Usman, H., Hamza, M. M., and Isah, B. Y., Unsteady MHD micropolar flow and mass transfer past a vertical permeable plate with variable suction, *Int. J. Comput. Appl.*, vol. **33**, pp. 18–24, 2011.
- Vafai, K. and Kim, S. J., Fluid mechanics of the interface region between a porous medium and a fluid layer—An exact solution, *Int. J. Heat Fluid Flow*, vol. **11**, pp. 254–256, 1990.